

LLS and FTIR Studies on the Hysteresis in Association and Dissociation of Poly(*N*-isopropylacrylamide) Chains in Water

He Cheng,[†] Lei Shen,[†] and Chi Wu*,^{†,‡}

The Hefei National Laboratory for Physical Sciences at Microscale, University of Science and Technology of China, Hefei, Anhui, China, and Department of Chemistry, The Chinese University of Hong Kong, Shatin, N.T., Hong Kong, China

Received November 30, 2005; Revised Manuscript Received January 19, 2006

ABSTRACT: Using a combination of static and dynamic laser scattering, we examined the association and dissociation of linear poly(*N*-isopropylacrylamide) (PNIPAM) chains in dilute aqueous solutions. There exists a hysteresis in the temperature dependence of the average hydrodynamic radius ($\langle R_h \rangle$), average radius of gyration ($\langle R_g \rangle$), and apparent weight-average molar mass ($M_{w,app}$) in one heating-and-cooling cycle. In the heating process, the chains first undergo intrachain contraction before interchain association to form stable aggregates at temperatures much higher than the lower critical solution temperature (LCST $\sim 32^\circ\text{C}$) of PNIPAM in water. In the cooling process before the solution temperature approaches the LCST, $M_{w,app}$ remains a constant and both $\langle R_g \rangle$ and $\langle R_h \rangle$ increase, but the ratio of $\langle R_g \rangle / \langle R_h \rangle$ decreases. In other words, the aggregates undergo an uneven swelling; namely, the periphery swells more than the center, and there is no chain dissociation. FTIR spectra reveal that as the temperature increases, the adsorption peak area related to the hydrogen bonding $\text{>C=O}\cdots\text{H-O-H}$ decreases, but the adsorption peak related to the hydrogen bonding $\text{>C=O}\cdots\text{H-N<}$ appears when the temperature is higher than the LCST, reflecting the dehydration and the formation of some additional intersegment hydrogen bonds in the collapsed state during the heating. Therefore, the chain contraction is entropy-driven, and the hysteresis can be attributed to these additional hydrogen bonds that act as the “cross-linking” points to make the chain aggregates behave like a “gel”. The chain dissociation only occurs when the temperature is much lower than the LCST, at which water becomes a very good solvent for PNIPAM.

Introduction

“Smart” polymers have some environmental responding properties so that they can swell or shrink corresponding to a small variation of temperature, pH, and ionic strength.^{1,2} Their potential applications in drug delivery, separation, and bioswitch have been widely suggested.³ Poly(*N*-isopropylacrylamide) (PNIPAM) is a typical example of such “smart” polymers, which can undergo the coil-to-globule transition in water at its low critical solution temperature (LCST $\sim 32^\circ\text{C}$).^{4–6} Note that such a transition of individual chains is rarely observed only for ultralong chains in extremely dilute solutions.⁷ One often faces a competition between intrachain contraction and interchain association, usually leading to macroscopic precipitation. Recently, some studies dealt with metastable aggregates (mesoglobules) made of a limited number of chains as well as the chain dissolution of these mesoglobules.^{8,9}

Wu and Wang observed a hysteresis in the cycle of the coil-to-globule-to-coil transition of individual long PNIPAM chain in extremely dilute aqueous solution. They attributed (or, more precisely, speculated) it to the formation of some additional hydrogen bonds in the collapsed state.¹⁰ Ding et al.¹¹ examined the association and dissolution of PNIPAM chains in water by using ultrasensitive differential scanning calorimetry (US-DSC) and found a hysteresis in one association–dissociation cycle. They also related it to some additional hydrogen bonds formed in the collapsed state. Maeda et al.^{12–15} found that, for those thermally sensitive polymers with a dissociable protein-like internal hydrogen bonding $\text{>C=O}\cdots\text{H-N<}$, increasing the solution temperature over the phase transition temperature resulted

in an intensity increase of the IR band at 1650 cm^{-1} assigned to the hydrogen bonding $\text{>C=O}\cdots\text{H-N<}$ but an intensity decrease of the IR band assigned to the hydrogen bonding $\text{>C=O}\cdots\text{H-O-H}$ (1625 cm^{-1}). On the other hand, for thermally sensitive polymers that are not able to form intrachain hydrogen bonding, such as poly(*N,N*-diethylacrylamide) (PDEA), increasing the temperature over the phase transition temperature can lead to an intensity increase of the IR band at 1635 cm^{-1} , which is assigned to free carbonyl groups, but an intensity decreases of the IR bands at 1619 and 1599 cm^{-1} , which are respectively assigned to the carbonyl group attached with one and two water molecules. However, there is no experimental correlation between the formation of $\text{>C=O}\cdots\text{H-N<}$ at higher temperatures and the observed hysteresis in the cooling process.

In the present study, we prepared relatively narrowly distributed PNIPAM chains by using the method developed before¹⁶ and investigated the temperature-induced in-situ association and dissociation of such PNIPAM chains in water by using FTIR and LLS. Note that a combination of these two methods enables us to examine the conformation and interaction of the PNIPAM chains during the microphase transition without any added probe. Our LLS and FTIR results confirmed the existence of a hysteresis in one heating-and-cooling cycle, which is attributed to the formation of some additional hydrogen bonds between the groups >C=O and H-N< only in the collapsed state. These intersegmental hydrogen bonds act as “the cross-linking” points among different chains so that each chain aggregate swells like a gel and the chain dissociation is delayed, which results in the observed hysteresis.

Experimental Section

Sample Preparation. *N*-Isopropylacrylamide (NIPAM) monomer from Aldrich was purified by a three-time recrystallization in

[†] University of Science and Technology of China.

[‡] The Chinese University of Hong Kong.

* The Hong Kong address should be used for all correspondence.

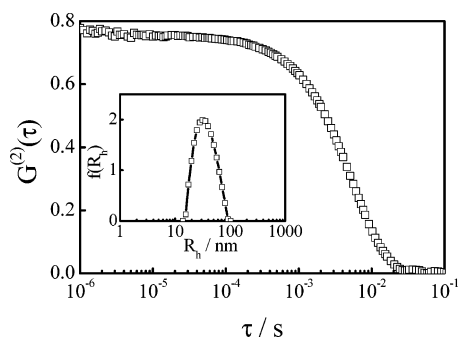


Figure 1. Typical normalized intensity–intensity time correlation function ($G^{(2)}(\tau)$) of PNIPAM chains in a dilute aqueous solution (2.3×10^{-4} g/mL) at $\theta = 15^\circ$ and $T = 25^\circ\text{C}$. The inset shows its corresponding intensity distribution of hydrodynamic radius ($f(R_h)$) calculated from the Laplace inversion of $G^{(2)}(\tau)$.

a mixture of benzene/*n*-hexane. Azobis(isobutyronitrile) (AIBN) was also recrystallized three times in methanol. In the synthesis of poly(*N*-isopropylacrylamide) (PNIPAM), 18.0 g of NIPAM was dissolved in 150 mL of benzene with 1 mol % of AIBN added as initiator. The solution mixture was degassed by three cycles of freezing and thawing. The polymerization was carried out in an oil bath at 56°C for 30 h under stirring and a positive nitrogen pressure. After the polymerization, benzene was removed by evaporation. The resulting crude polymer was further dried and then dissolved in acetone (500 mL). Hexane was added dropwise until the solution mixture slightly turned cloudy. The temperature was slightly raised to dissolve the PNIPAM chains and then slightly lowered to allow a very small fraction of longer PNIPAM chains to precipitate. The PNIPAM chains used in the present work were from the twelfth fractionation.

Laser Light Scattering. A commercial LLS spectrometer (ALV/SP-125) equipped with an ALV-5000 multitaup digital time correlator and a CW He–Ne laser (Uniphase, 22 mW at $\lambda = 632.8$ nm) was used. In static LLS, the angular dependence (15° – 150°) of the excess absolute time-averaged scattered intensity, i.e., the Rayleigh ratio $R_{90}(q)$, of a very dilute dispersion ($\sim 10^{-4}$ g/mL) can lead to the weight-averaged molar mass M_w and the z -averaged root-mean-square radius of gyration $\langle R_g \rangle_z^{1/2}$ (or written as $\langle R_g \rangle$) of scattering objects,¹⁷ where q is the scattering vector. In dynamic LLS, the Laplace inversion of each measured intensity–intensity time correlation function $G^{(2)}(t, q)$ can result in a line-width distribution $G(\Gamma)$.^{17,18} For a pure diffusive relaxation, Γ can be related to the translational diffusion coefficient D by $\Gamma/q^2 = D$ at $q \rightarrow 0$ and $C \rightarrow 0$ or a hydrodynamic radius $R_h = k_B T / (6\pi\eta D)$ with k_B , T , and η being the Boltzmann constant, the absolute temperature, and solvent viscosity, respectively.^{18,19}

Fourier Transform Infrared Spectroscopy. FTIR spectra were measured on a Nicolet Magna 750 IR spectrometer with a resolution of 4 cm^{-1} . In a typical experiment, 6 μL of PNIPAM in D_2O solution (0.012 g/mL) was added to a cell between two KRS-5 crystals (diameter 32 mm, thickness 3.5 mm) with a space of 20 μm . The IR cell was attached to a metal holder and heated by a heat tape. An electronic thermometer with a precision of $\pm 0.1^\circ\text{C}$ continuously monitored the temperature of the cell holder.

Results and Discussion

Figure 1 shows a typical intensity–intensity time correlation function ($G^{(2)}(\tau)$) of the PNIPAM chains in dilute aqueous solution (2.3×10^{-4} g/mL) at $\theta = 15^\circ$ and $T = 25^\circ\text{C}$. The inset shows its corresponding hydrodynamic radius distribution ($f(R_h)$) calculated from $G^{(2)}(\tau)$ by using a Laplace inversion program (CONTIN) in the correlator. The relative width of the line-width distribution, defined as $(\mu_2/\langle \Gamma \rangle^2 = \int_0^\infty G(\Gamma)(\Gamma - \langle \Gamma \rangle)^2 d\Gamma / \langle \Gamma \rangle^2)$, is ~ 0.1 , leading to an estimate of the polydispersity index ($M_w/M_n \approx 1.4$).²⁰ On the basis of Figure 1, we determined that the average hydrodynamic radius ($\langle R_h \rangle$) is 31

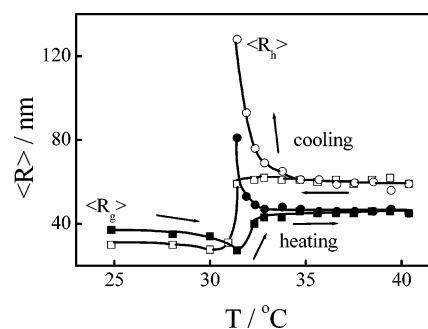


Figure 2. Temperature dependence of average hydrodynamic radius ($\langle R_h \rangle$) and radius of gyration ($\langle R_g \rangle$) of PNIPAM chain aggregates in one heating-and-cooling cycle.

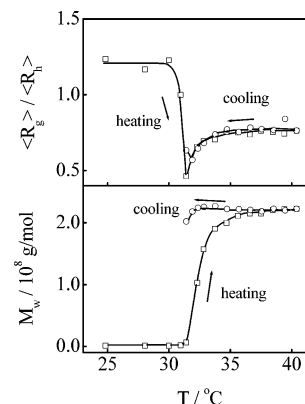


Figure 3. Temperature dependence of the ratio of average radius of gyration to average hydrodynamic radius ($\langle R_g \rangle / \langle R_h \rangle$) and weight-average molar mass (M_w) of PNIPAM chain aggregates in one heating-and-cooling cycle.

nm, and the apparent molecular weight-average molar mass ($M_{w,app}$) of it is 1.3×10^6 g/mol, where the subscript “app” is due to the uncorrected concentration effect, which should be small for such a dilute solution.

Figures 2 and 3 shows the temperature dependence of the average hydrodynamic radius ($\langle R_h \rangle$), the average radius of gyration ($\langle R_g \rangle$), their ratio, and the apparent weight-average molar mass ($M_{w,app}$) in one heating-and-cooling cycle. It is generally known or believed that water molecules exist in two different forms in water-soluble polymer solutions, namely, the bound and free water.^{21,22} The former is related to the chain hydration and affects its conformation. Before the temperature reaches the LCST of PNIPAM in the heating, both $\langle R_g \rangle$ and $\langle R_h \rangle$ decrease due to possible dehydration of the PNIPAM chains, showing the coil-to-globule transition of individual chains because $M_{w,app}$ remains a constant. In this temperature range, $\langle R_g \rangle$ decreases faster than $\langle R_h \rangle$ because they are defined in different ways; namely, $\langle R_g \rangle$ reflects the density distribution of the chain in real physical space, while $\langle R_h \rangle$ is the radius of a hard sphere with the same translational diffusion coefficient under the same condition. The slow decrease of $\langle R_h \rangle$ can be attributed to the decrease of the chain draining when it becomes more compact. A further increase of the temperature leads to the increase of $M_{w,app}$, i.e., the chain association. Note that both $\langle R_g \rangle$ and $\langle R_h \rangle$ increase, and each of them approaches a constant at high temperatures, indicating that stable aggregates are formed.^{23,24} The solution remained clear, and no macroscopic precipitation was observed for a long time.

On the other hand, the cooling leads to a more complicated process. In the initial stage of the cooling, there are no change in $M_{w,app}$, $\langle R_g \rangle$, and $\langle R_h \rangle$, which is expected because water is a nonsolvent at higher temperatures. As the solution temperature

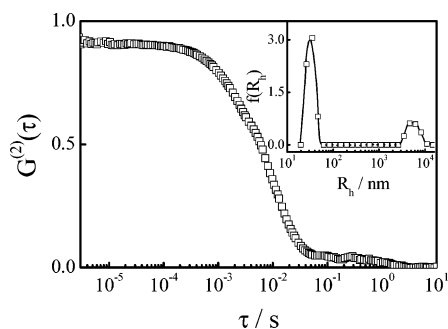


Figure 4. Typical normalized intensity–intensity time correlation function ($G^{(2)}(\tau)$) of PNIPAM chains in dilute aqueous solution (2.3×10^{-4} g/mL) at $\theta = 15^\circ$ after the solution was cooled from 40 to 30.4 °C. The inset shows its corresponding intensity distribution of hydrodynamic radius ($f(R_h)$) calculated from the Laplace inversion of $G^{(2)}(\tau)$ by using a CONTIN program in the correlator.

decreases and approaches the LCST, $M_{w,app}$ still remains a constant, but $\langle R_g \rangle$ and $\langle R_h \rangle$ start to sharply increase, revealing the swelling of the chain aggregates, but no chain dissociation. The swelling instead of the dissociation shows that some interchain interaction must be formed in the collapsed state at higher temperatures. Here, the hysteresis is more obvious than that in the single-chain folding.¹⁰ Further decrease of the solution temperature leads to the dissolution of most of the aggregates and the hysteresis disappears. We will come back to this point later.

The conformation change and the chain association/dissociation of polymer chains can be better viewed in terms of the ratio of $\langle R_g \rangle / \langle R_h \rangle$. As shown in Figure 3, during the heating process before the solution temperature reaches $\sim 30^\circ\text{C}$, both $\langle R_g \rangle / \langle R_h \rangle$ and M_w remain constants. A combination of Figures 2 and 3 clearly reveals that the chains undergo intrachain contraction, presumably due to the dehydration, but the coil conformation remains. Further increase of the temperature in the range ~ 30 – 31.5°C leads to a dramatic decrease of $\langle R_g \rangle / \langle R_h \rangle$ from ~ 1.35 to ~ 0.5 , but no significant change of M_w . It reveals that the collapse of individual chains results in a compact “core” and a relatively loose periphery made of many small intrachain loops. The increase of M_w in the range ~ 32 – 36°C clearly reveals interchain association. It should be noted that in this range $\langle R_g \rangle / \langle R_h \rangle$ increases from ~ 0.5 to ~ 0.8 , indicating that interchain association results in more uniform aggregates.²⁵ On the other hand, the collapse of small loops in the periphery also leads to a more uniform structure. The plateaus of both M_w and $\langle R_g \rangle / \langle R_h \rangle$ at higher temperatures indicate that interchain association stops. As expected, in the initial cooling stage, there is nearly no change in $\langle R_g \rangle / \langle R_h \rangle$. As the temperature approaches $\sim 34^\circ\text{C}$, $\langle R_g \rangle / \langle R_h \rangle$ starts to decrease, but M_w remains a constant. A combination of Figures 2 and 3 reveals that in this temperature range there is no dissolution, but the swelling of the aggregates is not uniform; namely, the periphery swells first, and the aggregates become the “core–shell” particles again. At $\sim 31^\circ\text{C}$, the decrease of M_w reveals the beginning of chain dissolution, and at the same time, $\langle R_g \rangle / \langle R_h \rangle$ starts to increase, reflecting the swelling of the core and the aggregates become more uniform.

Note that in Figures 2 and 3 there are no data at lower temperatures in the cooling process. This is because further decrease of the solution temperature leads to an additional slow mode in the measured time correlation function, as shown in Figure 4, where $\theta = 15^\circ$ and $T = 30.4^\circ\text{C}$. Such a slow mode cannot be completely removed even when the solution was cooled to 25°C . There are two possibilities: dust particles (but

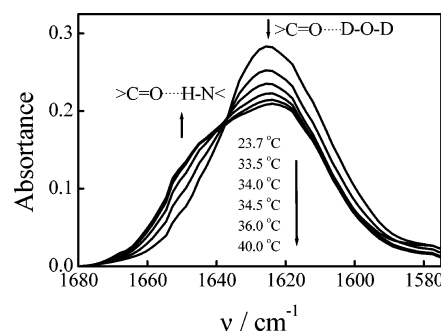


Figure 5. Temperature dependence of Fourier transform infrared spectroscopy (FTIR) of PNIPAM chains in a dilute aqueous solution (1.2×10^{-2} g/mL).

it is unlikely because the scattering cell was closed during the heating and cooling cycle) or a very small number of highly swollen large chain aggregates (more precisely, loose chain entanglements) which cannot be dissolved even when water becomes a good solvent. To test it, we put the sample cell at 4°C for 24 h and measured it again at 25°C . We found that the slow mode was gone. Therefore, Figure 4 reveals that the interchain interaction formed in the collapsed state is quite strong and can only be removed when water becomes an extremely good solvent. This is different from the intrachain association (folding) of individual chains.¹⁰

Previously, the clear hysteresis in the heating and cooling cycle was also observed in the swelling of PNIPAM brushes.²⁶ It was attributed to the formation of some additional intra- and interchain hydrogen bonds in the collapsed state without any evidence. It has been believed that some of these hydrogen bonds could persist in the cooling, especially when the temperature is not far away from the phase transition temperature. To confirm this speculation, we measured the temperature dependence of the FTIR spectra of PNIPAM chains by following a previous procedure^{12–14} and compare them with our LLS results. Here D_2O instead of H_2O was used so that the overlapping of the amide I band of PNIPAM moiety with the O–H bending band of water around 1640 cm^{-1} can be masked. Another reason is that D_2O can form a stronger hydrogen bond than H_2O even though their bond lengths are similar.²⁴

Figure 5 shows the FTIR spectra of PNIPAM in the range 1680 – 1560 cm^{-1} at different temperatures. The shoulder at 1650 cm^{-1} is attributed to the hydrogen bonding ($\text{>C=O}\cdots\text{H-N}<$), while the band centered at 1625 cm^{-1} is related to the hydrogen bonding ($\text{>C=O}\cdots\text{D-O-D}<$).^{12–14} As the solution temperature increases, the decrease of the weighting of the band at 1625 cm^{-1} reveals the dehydration, and at the same time, the increase of the shoulder weight at 1650 cm^{-1} shows that the formation of some hydrogen bonds between >N-H and $\text{O=C}<$. Obviously, the dehydration leads to intrachain contraction. The overlapping of the chain segments facilitates the formation of the hydrogen bonding between >N-H and $\text{O=C}<$. Note that the formation of the hydrogen bond $\text{>C=O}\cdots\text{H-N}<$ is entropically favored in comparison with the formation of $\text{>C=O}\cdots\text{D-O-D}<$ because the releasing of D_2O leads to higher translational entropy.

Assuming that each $\text{>C=O}\cdots\text{D-O-D}<$ bond and each $\text{>C=O}\cdots\text{H-N}<$ bond contribute a similar intensity in IR, we estimated the degree of dehydration and the molar fraction of intra- and interchain hydrogen bonds from the ratio of the peak areas ($f_A = A(1650)/[A(1650) + A(1625)]$), where the two Gaussian peaks were obtained by using a nonlinear fitting of the overlapped amide I region in the spectrum. Figure 6 shows

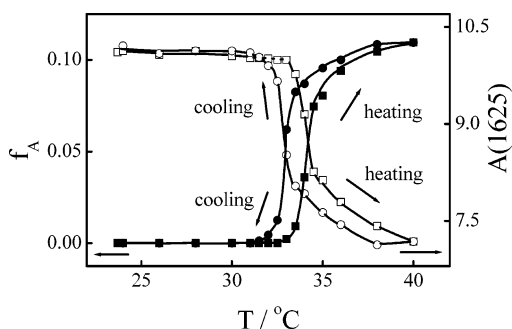


Figure 6. Temperature dependence of the area ratio ($f_A = A(1650)/[A(1650) + A(1625)]$) of the peaks centered at 1650 and 1625 cm^{-1} , which reflects the molar ratio of intra- and interchain hydrogen bonds ($\text{>C=O}\cdots\text{H-N<}$) formed in the collapsed state during the heating, and the area of the peak centered at 1625 cm^{-1} , which reflects the degree of dehydration, during one heating-and-cooling cycle.

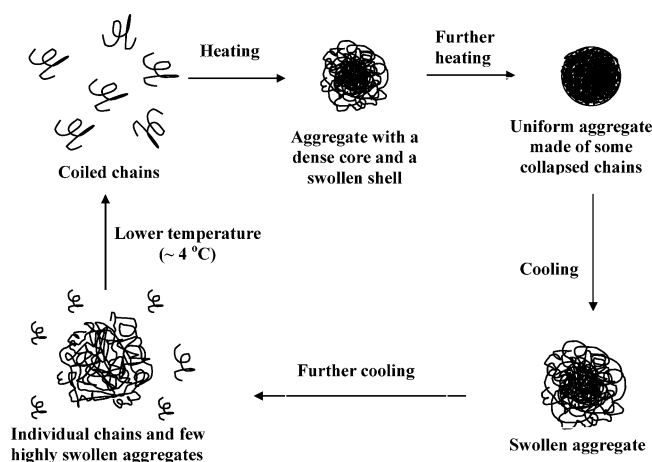


Figure 7. Schematic of chain association and dissolution of PNIPAM in water during one heating-and-cooling cycle.

that the temperature dependence of f_A and $A(1625)$ in one heating-and-cooling cycle. f_A is close to zero, and $A(1625)$ slightly decreases in the heating process when the solution temperature is lower than the LCST of PNIPAM. They clearly reveal that intra- and interchain hydrogen bonds ($\text{>C=O}\cdots\text{H-N<}$) are formed only when the PNIPAM chains start to collapse because in the collapsed state, intrachain and interchain overlapping of different segments is enhanced. On the other hand, f_A approaches a constant smaller than 11% at higher temperatures, presumably that the chains are “frozen” in their fully collapsed state so that the formation of more hydrogen bonds between >C=O and H-N< practically stops. It shows that even in the fully collapsed state, most >C=O groups still form the hydrogen bonds with D_2O . Note that no macroscopic precipitation was observed.

As shown in Figure 6, the hysteresis in one heating-and-cooling cycle is very clear. At the same temperature, f_A and $A(1620)$ in the cooling process are always larger and smaller, respectively, than those values in the heating unless the solution temperature is below $\sim 30^\circ\text{C}$. It clearly reveals that the hysteresis is due to the formation of intra- and interchain hydrogen bonds between different chain segments when they are overlapped in the collapsed state. Such formed hydrogen bonds cannot be completely removed in the cooling process even when water becomes a good solvent; i.e., the temperature is lower than the LCST. Figure 7 schematically summarizes the association and dissolution of the PNIPAM chains in dilute aqueous solutions in one heating-and-cooling cycle.

Conclusion

The hysteresis observed in the association and dissolution of thermally sensitive polymer, poly(*N*-isopropylacrylamide) (PNIPAM), during one heating-and-cooling cycle was studied by a combination of LLS and FTIR. Our results showed that the >C=O groups in PNIPAM are bound to water via the hydrogen bonding at lower temperatures, and there is nearly no intrachain hydrogen bonding between >C=O and H-N< . The heating from the room temperature to the LCST ($\sim 32^\circ\text{C}$) only leads to a slight dehydration. The dehydration really starts when the solution temperature is higher than the LCST. During the dehydration, some of the >C=O groups start to form inter- and intrachain hydrogen bonding with the H-N< groups. Some of these hydrogen bonds remain during the cooling even when the temperature is below the LCST. These remaining hydrogen bonds act as the “cross-linking” points inside the swollen chain aggregates. This is why the chain aggregates swell, but not dissociate, even when the solution temperature is lower than, but not far away from, the LCST. The incompletely removal of those interchain hydrogen bonds formed in the collapsed state during the dehydration is the exact reason behind the observed hysteresis. We have confirmed the previous speculation about the hysteresis observed in the coil-to-globule transition of individual PNIPAM chains. Note that at sufficiently lower temperatures the hysteresis can be completely removed. Different heating–cooling cycles led to the same results. Such a hysteresis should be general phenomena for water-soluble polymer chains that can form intersegmental hydrogen bonds. It would be very interesting to see whether there also exists such a hysteresis for other thermally sensitive polymer chains without any possible interchain hydrogen bonding.

Acknowledgment. The financial support of the National Natural Science Foundation of China (20274045, 50025309, and 90201016), the Chinese Academy of Sciences (KJCX2-SW-H14), and the Research Grants Council of the Hong Kong Special Administration Region Earmarked Grant 2003/04 (CUHK4029/03P, 2160206) is gratefully acknowledged.

References and Notes

- Bignotti, F.; Penco, M.; Sartore, L.; Peroni, I.; Mendichi, R.; Casolaro, M.; Amore, A. D. *Polymer* **2000**, *41*, 8247.
- Burova, T. V.; Ginberg, N. V.; Grinberg, V. Y.; Kalinina, E. V.; Lozinsky, V. I.; Aseyev, V. O.; Holappa, S.; Tenhu, H.; Khokhlov, A. R. *Macromolecules* **2005**, *38*, 1292.
- Okano, T.; Kikuchi, A.; Sakurai, Y.; Takei, Y.; Ogata, N. *J. Controlled Release* **1995**, *36*, 125.
- Otake, K.; Inomata, H.; Konno, M.; Saito, S. *Macromolecules* **1990**, *23*, 283.
- Kubota, K.; Hamano, K.; Kuwahara, N.; Fujishige, S.; Ando, I. *Polym. J.* **1990**, *22*, 1051.
- Kubota, K.; Fujishige, S.; Ando, I. *J. Phys. Chem.* **1990**, *94*, 5154.
- Wu, C.; Zhou, S. Q. *Phys. Rev. Lett.* **1996**, *77*, 3053.
- Siu, M.; Liu, H. Y.; Zhu, X. X.; Wu, C. *Macromolecules* **2003**, *36*, 2103.
- Wu, C.; Li, W.; Zhu, X. X. *Macromolecules* **2004**, *37*, 4989.
- Wu, C.; Wang, X. H. *Phys. Rev. Lett.* **1998**, *79*, 4092.
- Ding, Y. W.; Ye, X. D.; Zhang, G. Z. *Macromolecules* **2005**, *38*, 904.
- Maeda, Y.; Higuchi, T.; Ikeda, I. *Langmuir* **2000**, *16*, 7503.
- Maeda, Y.; Yanamoto, H.; Ikeda, I. *Colloid Polym. Sci.* **2004**, *282*, 1268.
- Maeda, Y.; Higuchi, T.; Ikeda, I. *Langmuir* **2001**, *17*, 7535.
- Maeda, Y.; Nakamura, T.; Ikeda, I. *Macromolecules* **2002**, *35*, 10172.
- Zhou, S. Q.; Fan, S. Y.; Steve, C. F.; Au, Y.; Wu, C. *Polymer* **1995**, *36*, 1341.
- Chu, B.; Wang, Z.; Yu, J. *Macromolecules* **1991**, *24*, 6832.
- Wu, C.; Xia, K. Q. *Rev. Sci. Instrum.* **1994**, *65*, 587.
- Wu, C.; Zhou, S. Q. *J. Polym. Sci., Polym. Phys.* **1996**, *34*, 1597.
- Akcasu, Z.; Han, C. C. *Polymer* **1981**, *22*, 1019.

- (21) Corkhill, P. H.; Jolly, A. M.; Ng, C. O.; Tighe, B. J. *Polymer* **1987**, 28, 1758.
- (22) Barnes, A.; Corkhill, P. H.; Tighe, B. J. *Polymer* **1988**, 29, 2191.
- (23) Kujawa, P.; Winnik, F. M. *Macromolecules* **2001**, 34, 4030.
- (24) Laukkanen, A.; Valtola, L.; Winnik, F. M.; Tenhu, H. *Macromolecules* **2004**, 37, 2268.
- (25) Zhou, C. L.; Zhao, Y.; Jao, T. C.; Wu, C.; Winnik, M. A. *J. Phys. Chem. B* **2002**, 106, 9514.
- (26) Liu, G. M.; Zhang, G. Z. *J. Phys. Chem. B* **2005**, 109, 743.

MA052561M